



TEMPERATURE DEPENDENT SPECTRAL RESPONSE MEASUREMENTS FOR III-V MULTI-JUNCTION SOLAR CELLS

Daniel Aiken, Mark Stan, Chris Murray, Paul Sharps, Jenifer Hills, and Brad Clevenger
Emcore Photovoltaics, 10420 Research Rd. SE, Albuquerque, NM 87123

ABSTRACT

Temperature coefficients for the integrated current of all three subcells in a production InGaP/InGaAs/Ge solar cell structure have been measured at temperatures ranging from 5°C to 100°C. The InGaP, InGaAs, and germanium temperature coefficients are 0.011, 0.009, and 0.044 mA/cm²/°C, respectively. This data can be used to design multi-junction solar cells for optimum performance at any specified operating temperature in this range. The predicted current mismatch for a similar triple junction operating at 100°C but designed to be current matched at 28°C is approximately 3%.

INTRODUCTION

Monolithic, series interconnected group III-V multi-junction solar cells have been used to provide space power for near-earth orbits as well as interplanetary missions such as deep space 1 [1] and Mars lander. Their feasibility is also being evaluated for near-sun missions as well as in high-concentration receivers for terrestrial power generation [2]. This wide range of environments results in operating temperatures from sub-zero to over 100°C.

The series interconnected design of these solar cells implies that subcell current matching is imperative for achieving the highest possible performance. Furthermore, the spectrum splitting characteristic of these devices implies that individual subcells convert a relatively narrow range of spectral wavelengths into photocurrent, as compared to silicon solar cells, for example. This makes multi-junctions much more sensitive to changes in either the illumination spectrum (AM0, AM1.5D, etc.) or their spectral response characteristics (as would occur with changes in temperature). The relatively wide range of operating temperatures coupled with the increased sensitivity to spectral shifts requires a thorough understanding of the temperature characteristics of these devices.

A common requirement in typical space qualification procedures is measurement of the current-voltage parameter temperature coefficients, e.g. dJ_{sc}/dT . This data is valuable in establishing the solar cell performance versus temperature, but offers little in terms of physical insight and design feedback. Knowledge of how each subcell's spectral response changes with temperature provides useful design information for optimizing cell per-

formance under any illumination spectrum and at any operating temperature.

EXPERIMENTAL

Spectral response measurements have been performed on each of the subcells in Emcore's production InGaP/InGaAs/Ge triple junction solar cell design. These measurements were performed on bare 4cm² triple junctions. Convolution with the ISO-standard AM0 spectrum then yielded an integrated current density, which is a good estimate of each subcell's short circuit current when all the subcell device characteristics are reasonably close to ideal. A relationship between integrated current and temperature was then established for each subcell in the triple junction.

Measurement hardware included a quartz-tungsten-halogen light source chopped at 167 or 221 Hz and filtered through a single grating monochromator with a 2nm (InGaP and InGaAs subcells) or 3nm (germanium subcell) half bandwidth wavelength resolution. Slit widths for measurements on the top (InGaP) and middle (InGaAs) subcells were chosen in a compromise between wavelength resolution and signal strength. The resolution of measurements made on the bottom (germanium) subcell was limited to 3nm by long wavelength grating dispersion and the minimum available slit width. The narrow bandwidths were chosen to allow high-resolution (1nm step) scans near the band edge of each subcell.

The devices were underfilled by an approximately 5mm diameter monochromatic beam. Devices were vacuum mounted on a gold coated brass stage. Thermoelectric elements were sandwiched between the brass stage and a water cooled/heated aluminum block. Temperature measurements were made at the back of the device via a spring loaded calibrated thermocouple, as well as at the center of the brass stage using an embedded thermocouple.

A 75 Watt focused quartz tungsten halogen light source was used to light bias the device under test. Spectrally selective light biasing was achieved with commonly available optical filters. The effective shunt resistance of each subcell in the multi-junction was measured *a priori* using the spectrally selective light bias and a curve tracer. Only solar cells with near-ideal diode behavior and a high effective shunt resistance in all subcells were tested. This screening technique eliminates the need for voltage biasing, minimizes thermal noise generated by shunt or leaky devices, and provides measure-

ment accuracy by assuring that the effective shunt resistance of the device is at least 2 orders of magnitude greater than the amplifier input impedance.

Spectral response data was collected for devices operating in an air ambient and at temperatures ranging from 5°C to 100°C. Temperatures below approximately 10°C required a nitrogen shower to prevent water condensation on the device.

RESULTS

InGaP top subcell

Figure 1 shows the quantum efficiency (QE) of the top (InGaP) subcell. Clearly evident in the figure is a red shift in the band edge response (650-700nm) as the temperature is increased. The data also suggests a less pronounced red shift at wavelengths less than 500nm. This is presumably caused by a decrease in the bandgap of the window layer material with temperature, resulting in increased parasitic absorption in the window layer as the temperature is increased.

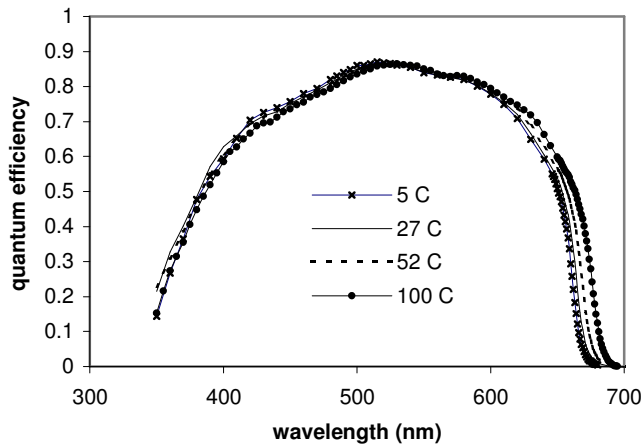


Fig. 1 Quantum efficiency of the InGaP subcell as a function of temperature.

The measurements were conducted using 1nm wavelength steps near the band edge such that small shifts in the spectral response could be accurately measured. Shown in Figure 2 is the derivative of the QE data, which was used to quantify the relative change in the band edge as a function of temperature. The band edge for each QE curve is defined here as the midpoint of the half bandwidth of the QE derivative. The resulting number loosely correlates with the peak of the QE derivative, which is otherwise difficult to identify when significant scatter is present in the data. Due to the scatter in the data and the hardware-limited wavelength resolution, the accuracy of this technique is estimated to be +/- 1nm in this case.

Figure 3 shows a linear fit of band edge wavelength versus temperature as determined here using Figure 2. Figure 3 also shows a linear fit of photoluminescence (PL) data as published by Lu et al. [3]. All linear fits presented here were calculated using the least squares approximation. Figure 3 suggests very good agreement between the slope of the two linear fits. The difference in the y-

intercept is most likely due to differing degrees of group-III sublattice ordering [4] and/or small differences in the alloy composition of the two materials.

Despite the crude, non-physical nature of this band edge determination technique, Figure 3 suggests good absolute agreement with the PL wavelength measured in-house at room temperature, and good rate-of-change agreement with published PL versus temperature data from Lu et al. This agreement supports the accuracy and validity of these spectral response measurements for determining the photoresponse characteristics of these solar cells as a function of temperature.

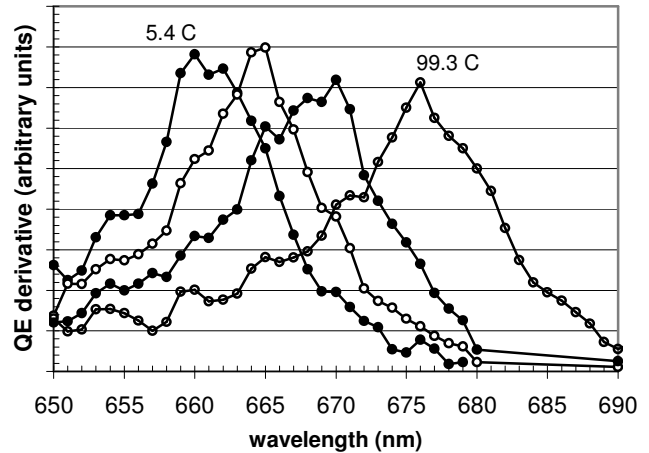


Fig. 2 InGaP subcell quantum efficiency derivative used to determine the relative band edge shift with temperature.

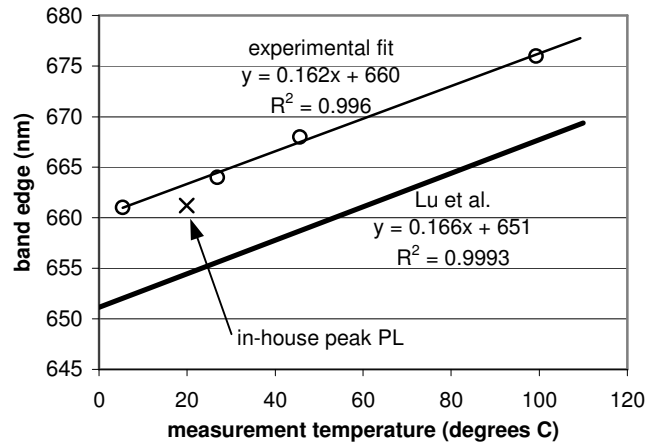


Fig. 3 A linear fit of band edge data measured experimentally using spectral response data, as compared to both a linear fit of published PL data for $\text{In}_{0.5}\text{Ga}_{0.5}\text{P}$ [3] and PL wavelength measured in-house at room temperature.

Shown in Figure 4 is the AM0 integrated current density for the InGaP subcell, along with two linear fits. Inclusion of the datapoint at 100C resulted in a poor linear fit, which suggests that this datapoint may be anomalous or that a linear fit is not appropriate. Under the assumption that a linear fit is most appropriate, a second linear fit is

therefore provided based on only the first three data-points. This second fit correlates well with dJ_{SC}/dT data measured in-house under solar simulation.

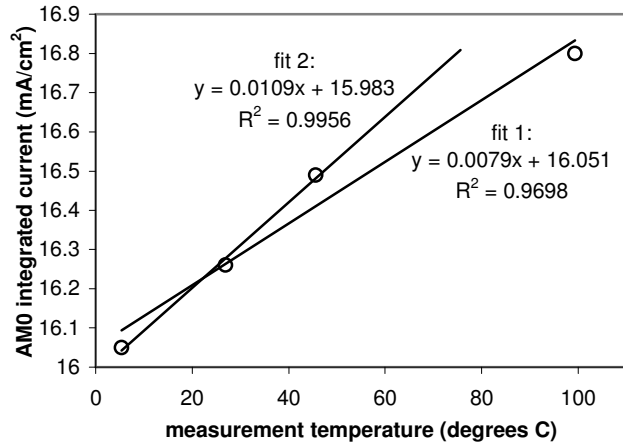


Fig. 4 AM0 integrated current as a function of temperature for the InGaP subcell, along with two linear fits of the experimental data.

InGaAs middle subcell

Figure 5 shows the quantum efficiency of the InGaAs subcell for various temperatures. The difference in the leading edge and trailing edge characteristics suggests that the temperature dependence of the InGaAs subcell band edge is greater than that of the InGaP subcell.

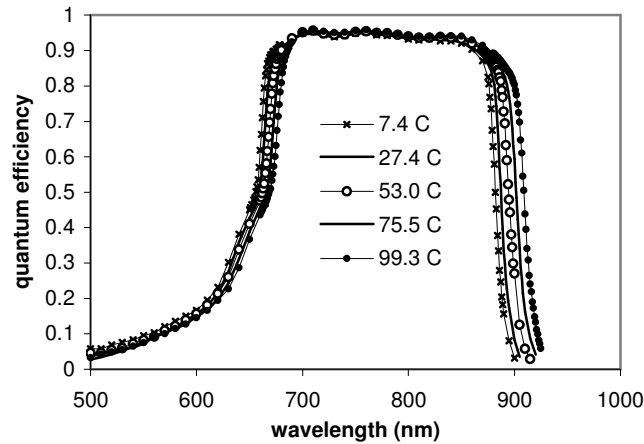


Fig. 5 Quantum efficiency of the InGaAs subcell as a function of temperature.

Figure 6 shows the band edge as a function of temperature for the InGaAs subcell as determined using the QE derivative method discussed previously. Good agreement is evident between the slope of the two linear fits. The difference in intercept between the linear fit of Blakemore's GaAs data [5] and the experimental InGaAs fit can be used to calculate the mol fraction of Indium in the InGaAs middle subcell. The result is an approximately 0.02 indium mol fraction using ternary bandgap data from

Adachi [6]. This agrees well with band edge data measured in-house using PL.

Figure 7 shows the AM0 integrated current density for the InGaAs subcell as a function of temperature, along with a linear fit of the data.

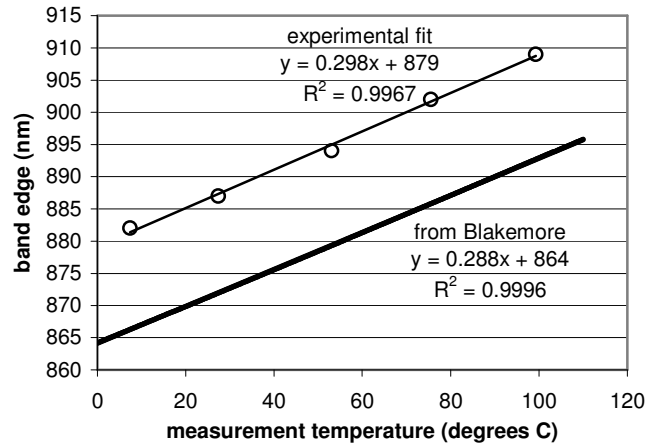


Fig.6 A linear fit of InGaAs band edge data determined experimentally using spectral response data, as compared to a linear fit of published bandgap data for GaAs [5].

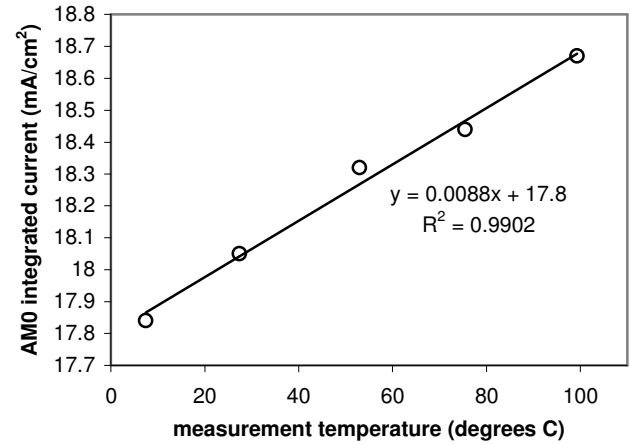


Fig. 7 AM0 integrated current as a function of temperature for the InGaP subcell, along with a linear fit of the experimental data

Germanium bottom subcell

Figure 8 shows the quantum efficiency of the germanium subcell for various temperatures. Evident in the figure is a red shift in the long wavelength response that starts at the germanium direct band edge wavelength of 1550nm (at room temperature) and continues towards the indirect band edge wavelength of 1850nm (at room temperature).

Also of interest is the increasing spectral response with temperature at wavelengths between 950 and 1500nm. Three possible explanations of this trend include a change in the absorption characteristics of the germanium subcell (as would result from a shift in AR

coating properties with temperature), a change in the collection efficiency of this subcell, or a measurement artifact. Due to the difficulty in achieving absolute spectral response measurements for the germanium subcell, we assume this characteristic is a measurement artifact until proven otherwise. A potential explanation of this effect is related to the long wavelength photoresponse of the germanium subcell. Heating the test stage creates an increasingly intense source of long wavelength photons that are converted by the germanium subcell. This changes the relative bias point of the solar cell during the spectral response measurement. If this bias point is located at a sufficiently non-linear portion of the I-V curve, an anomalous, temperature dependent spectral response could result. Additional experimentation is necessary to resolve this issue.

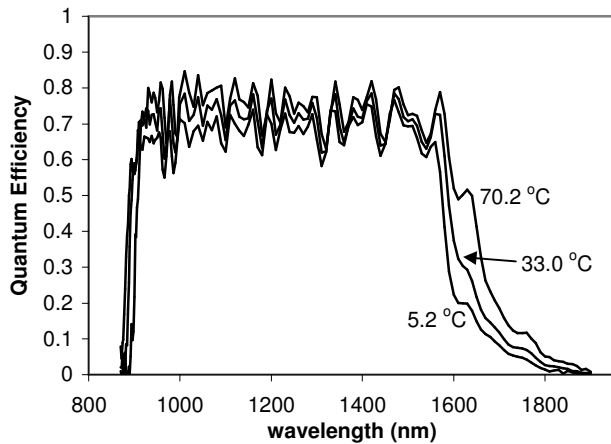


Fig. 8 Quantum efficiency of the germanium subcell as a function of temperature.

CONCLUSIONS

The linearly fitted, AM0 integrated current density temperature coefficients are summarized in Table 1. Good agreement was obtained between experimentally determined band edge wavelengths and independent PL wavelength measurements. Good correlation was also achieved between the InGaP topcell temperature coefficient and the triple junction current density temperature coefficient dJ_{SC}/dT . These numbers should be well-correlated because these triple junctions are topcell current limited at beginning-of-life.

Table 1. Summary of linear fit data determined from spectral response measurements at various temperatures.

subcell	Slope ($\text{mA}/\text{cm}^2/^\circ\text{C}$)	y-int (mA/cm^2)
InGaP (fit2)	0.011	15.98
InGaP (fit1)	0.008	16.05
InGaAs	0.009	17.80
germanium	0.044	23.16

Inspection of Figure 5, as well as published bandgap versus temperature data, suggests that the band edge in InGaAs is much more sensitive to temperature than the

InGaP subcell. This is partially compensated by the fact that both the leading edge and the trailing edge of the InGaAs middle cell spectral response shift to the red with increasing temperature. The result is a solar cell that is fairly insensitive to temperature in terms of photogeneration and current matching. As an example, a triple junction designed to be current matched at 28°C and generating 17 mA/cm^2 short circuit current is current mismatched by only 3.3% at 100°C.

Additionally, the apparently high temperature coefficient of 0.044 $\text{mA}/\text{cm}^2/^\circ\text{C}$ for the germanium subcell suggests that this subcell will generate sufficient current at all temperatures in this range so as not to become current limiting.

These coefficients do not apply to solar cells with spectral response characteristics degraded in a radiation environment. However, because typical radiation energies and fluences degrade the red response of the InGaAs middle subcell, it is plausible to expect the integrated current temperature coefficient of the middle subcell to decrease with radiation dose. This in turn would make these cells less temperature sensitive than in the beginning-of-life case examined here.

REFERENCES

- [1] M.J. O'Neill, A.J. McDanal, M.F. Piszczor, M.I. Eskenazi, C. Carrington, D.L. Edwards, and H.W. Brandhorst, "The Stretched Lens Ultralight Concentrator Array", *Twenty-Eighth IEEE PVSC*, 2000, pp. 1135-1138.
- [2] M.J. O'Neill, A.J. McDanal, H.L. Cotal, R. Sudharasan, D.D. Krut, J.H. Ermer, N.H. Karam, D.R. Lillington, "Development of Terrestrial Concentrator Modules Incorporating High-Efficiency Multi-Junction Cells", *Twenty-Eighth IEEE PVSC*, 2000, pp. 1161-1164.
- [3] S.C. Lu, M.C. Wu, C.Y. Lee, and Y.C. Yang, "Temperature dependence of photoluminescence from Mg-doped $\text{In}_{0.5}\text{Ga}_{0.5}\text{P}$ grown by liquid-phase epitaxy", *J. Applied Physics*, **70**, 1991, pp. 2309-2312.
- [4] A. Gomyo, K. Kobayashi, S. Kawata, I. Hino, T. Suzuki, "Studies of $\text{Ga}_x\text{In}_{1-x}\text{P}$ Layers Grown by Metalorganic Vapor Phase Epitaxy; Effects of V/III Ratio and Growth Temperature", *J. Crystal Growth*, **77**, 1986, pp. 367-373.
- [5] J.S. Blakemore, "Semiconducting and Other Major Properties of GaAs" *J. Applied Physics*, **53**, 1982, pp. R123-181.
- [6] S. Adachi, *Physical Properties of III-V Semiconductor Compounds*, J. Wiley & Sons, 1992.